

Microstructural development in equiatomic multicomponent alloys

B. Cantor, I.T.H. Chang*, P. Knight, A.J.B. Vincent

*Department of Materials, Oxford University, Parks Road, Oxford OX1 3PH, UK
School of Metallurgy and Materials, Birmingham University, Birmingham B15 2TT, UK*

Abstract

Multicomponent alloys containing several components in equal atomic proportions have been manufactured by casting and melt spinning, and their microstructures and properties have been investigated by a combination of optical microscopy, scanning electron microscopy, electron probe microanalysis, X-ray diffractometry and microhardness measurements. Alloys containing 16 and 20 components in equal proportions are multiphase, crystalline and brittle both as-cast and after melt spinning. A five component $\text{Fe}_{20}\text{Cr}_{20}\text{Mn}_{20}\text{Ni}_{20}\text{Co}_{20}$ alloy forms a single fcc solid solution which solidifies dendritically. A wide range of other six to nine component late transition metal rich multicomponent alloys exhibit the same majority fcc primary dendritic phase, which can dissolve substantial amounts of other transition metals such as Nb, Ti and V. More electronegative elements such as Cu and Ge are less stable in the fcc dendrites and are rejected into the interdendritic regions. The total number of phases is always well below the maximum equilibrium number allowed by the Gibbs phase rule, and even further below the maximum number allowed under non-equilibrium solidification conditions. Glassy structures are not formed by casting or melt spinning of late transition metal rich multicomponent alloys, indicating that the confusion principle does not apply, and other factors are more important in promoting glass formation.

© 2003 Elsevier B.V. All rights reserved.

Keywords: Multicomponent alloys; Equiatomic; Casting

1. Introduction

Conventional strategy for developing metallurgical alloys is to select the main component based on a primary property requirement, and to use alloying additions to confer secondary properties. This strategy has led to many multicomponent alloys based on a single main component. Typical examples include Ni superalloys, wrought Al alloys and stainless steels. In a few cases two or three components are present in substantial proportions, e.g. the Cu–Zn brasses or Sn–Pb solders.

Conventional alloy development strategy leads to an enormous amount of knowledge about alloys based on one component, but to very little or no knowledge about alloys containing several main components in approximately equal proportions. Theories for the occurrence, structure and properties of crystalline phases are similarly restricted to alloys based on one or two main components. Information and understanding is highly developed about alloys close to the apexes and edges of the phase diagram, with

much less known about alloys in the centre of the diagram. This imbalance becomes rapidly much more pronounced as the number of components increases. For quaternary, quinary and higher order systems, information about alloys in the centre of the phase diagram is virtually non-existent. Since most of the possible alloy compositions are based on more than one component, it is clear that conventional alloy development strategy has been very restrictive in exploring the full range of possible alloys.

This paper describes an initial attempt to investigate the unexplored central region of multicomponent alloy phase space, concentrating particularly on multicomponent transition metal alloys which are found to exhibit a surprising degree of intersolubility in a single fcc phase.

2. Experimental

Approximately 10 g ingots of a wide variety of multicomponent alloys were made by induction melting pure elements in equal atomic proportions in an Al_2O_3 crucible under Ar. Some of the alloys were melt spun by remelting in quartz crucibles under Ar, and then ejecting with Ar at 14–21 kPa through a 1 mm orifice onto a Cu drum rotating at

* Corresponding author.

E-mail address: i.t.chang@bham.ac.uk (I.T.H. Chang).

15–40 ms⁻¹. Samples were sectioned and polished for microstructural and compositional characterisation and hardness testing, using an Olympus OM-2 optical microscope, Philips 501 scanning electron microscope (SEM), Cameca Camebax electron probe microanalyser (EPMA), Philips PW 1050 X-ray diffractrometer (XRD), and Vickers microhardness tester model UHT-1 with 10 g load.

3. Results

The first alloy investigated consisted of 20 elements in equal atomic proportions, i.e. 5 at.% each of Mn, Cr, Fe, Co, Ni, Cu, Ag, W, Mo, Nb, Al, Cd, Sn, Pb, Bi, Zn, Ge, Si, Sb, Mg. The second alloy consisted of 16 elements in equal atomic proportions, i.e. 6.25 at.% each of Mn, Cr, Fe, Co,

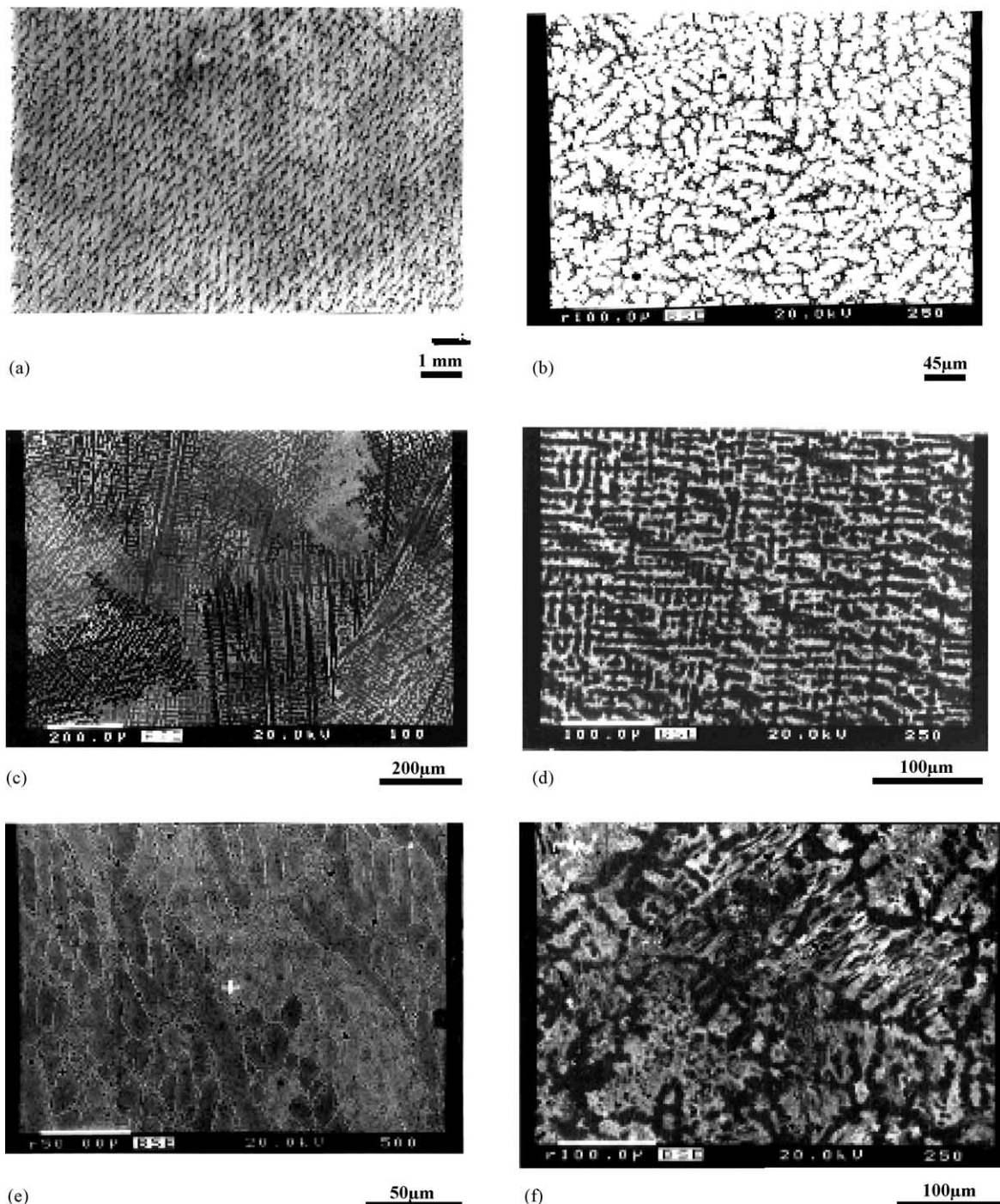


Fig. 1. (a) Optical micrograph of etched $\text{Fe}_{20}\text{Cr}_{20}\text{Mn}_{20}\text{Ni}_{20}\text{Co}_{20}$; SEM micrographs of (b) $\text{Fe}_{16.7}\text{Cr}_{16.7}\text{Mn}_{16.7}\text{Ni}_{16.7}\text{Co}_{16.7}\text{Nb}_{16.7}$; (c) $\text{Fe}_{16.7}\text{Cr}_{16.7}\text{Mn}_{16.7}\text{Ni}_{16.7}\text{Co}_{16.7}\text{Ge}_{16.7}$; (d) $\text{Fe}_{16.7}\text{Cr}_{16.7}\text{Mn}_{16.7}\text{Ni}_{16.7}\text{Co}_{16.7}\text{Cu}_{16.7}$; (e) $\text{Fe}_{16.7}\text{Cr}_{16.7}\text{Mn}_{16.7}\text{Ni}_{16.7}\text{Co}_{16.7}\text{Ti}_{16.7}$; and (f) $\text{Fe}_{16.7}\text{Cr}_{16.7}\text{Mn}_{16.7}\text{Ni}_{16.7}\text{Co}_{16.7}\text{V}_{16.7}$.

Table 1
Dendritic (D) and interdendritic (I) compositions (at.%)

Alloy	Region	Fe	Cr	Mn	Ni	Co	Nb	Ge	Cu	Ti	V
FeCrMnCoNi	D	20.2	20.5	19.4	19.5	20.4					
	I	16.1	27.0	23.0	17.0	17.0					
Nb	D	16.5	15.7	12.0	13.0	17.8	25.0				
	I	15.5	19.4	25.4	23.7	14.2	1.9				
Ge	D	21.7	21.0	12.0	13.5	19.2		12.6			
	I	8.9	11.0	20.3	22.3	13.5		24.0			
Cu	D	21.6	18.4	12.7	16.9	23.7			6.8		
	I	3.3	3.6	24.4	15.6	5.9			47.4		
Ti	D	19.7	7.3	14.3	13.5	20.5				24.8	
	I	18.4	10.1	24.0	22.7	15.9				8.9	
V	D	18.8	19.5	7.7	25.6	18.3					18.9
	I	18.4	16.4	8.0	21.5	19.6					16.2

Ni, Cu, Ag, W, Mo, Nb, Al, Cd, Sn, Pb, Zn and Mg, the same as the first alloy but without the semi-metals Bi, Ge, Si and Sb. Both alloys were multiphase and brittle, as-cast and after melt spinning. Surprisingly, however, the alloys consisted predominantly of a single fcc primary phase, containing many elements but particularly rich in transition metals, notably Cr, Mn, Fe, Co and Ni. In addition, there were a few interdendritic phases. Further investigation concentrated on exploring the multicomponent fcc single phase field, by manufacturing a five component alloy consisting of 20 at.% each of Cr, Mn, Fe, Co and Ni, as well as six, seven, eight and nine component alloys consisting of 16.7, 14.3, 12.5 and 11.1 at.% each, respectively, of the same five elements together with other elements such as Cu, Ti, Nb, V, W, Mo, Ta and Ge. This paper concentrates on the five component FeCrMnNiCo alloy, with 6th element additions of Nb, Ge, Cu, Ti and V.

Fig. 1 shows microstructures of (a) the as-cast five component FeCrMnNiCo alloy; and (b–f) the Nb, Ge, Cu, Ti and V alloys, respectively. All the alloys exhibited a dendritic microstructure, with the dendrite size and morphology varying from one alloy to another. The Ti, Nb and V alloys contained rounded dendrites with an average primary arm width of 20 µm, but the dendrites in the other alloys were more regular and highly branched. The average primary dendrite arm width was 15 µm in FeCrMnNiCo, but only 5 µm in the Cu alloy. The secondary dendrite arm spacing was also smaller in the Cu alloy. There was interdendritic segregation with no second phase in FeCrMnNiCo and the Cu alloy, but the Nb and Ti alloys showed a second interdendritic phase, and the V alloy exhibited multiphase interdendritic regions.

Dendritic and interdendritic compositions varied from one alloy to another, as listed in Table 1. The dendrite composition in FeCrMnNiCo consisted of equal proportions of Fe, Cr, Mn, Ni and Co, with an interdendritic composition low in Fe and high in Cr and Mn, as shown in the Fe X-ray map in Fig. 2. Table 1 shows that Nb and Ti segregate preferentially to the dendrites and are depleted in the interdendritic

regions; Ge and Cu segregate preferentially to the interdendritic regions and are depleted in the dendrites; and V partitions equally between the dendrites and the interdendritic regions. There was a slight tendency for Mn to segregate preferentially to the interdendritic regions in the six component alloys. A typical example can be seen in the Mn X-ray map from the Nb alloy in Fig. 3.

Fig. 4 shows XRD traces from: (a) the five component FeCrMnNiCo alloy; and (b–f) the Nb, Ge, Cu, Ti and V alloys, respectively. In all the alloys, the dendrites were fcc with a lattice parameter in the range 0.358–0.364 nm, as listed in Table 2. Minor interdendritic bcc and other phases were present in the Ge, Ti and V alloys.

Table 3 gives dendritic and interdendritic microhardness values. Dendritic and interdendritic hardnesses were 300

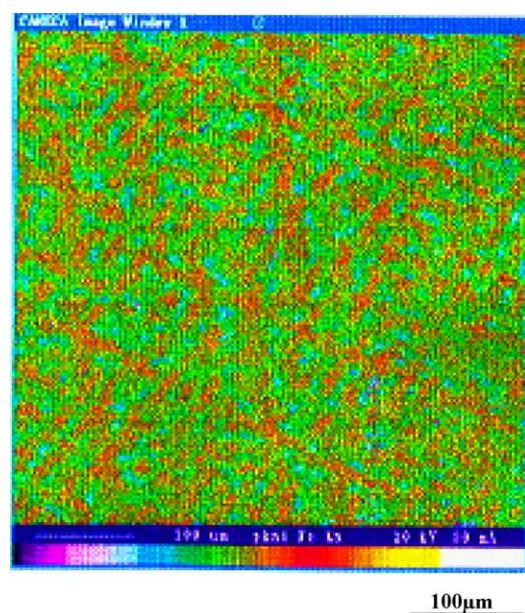


Fig. 2. Fe X-ray map from Fe₂₀Cr₂₀Mn₂₀Ni₂₀Co₂₀.

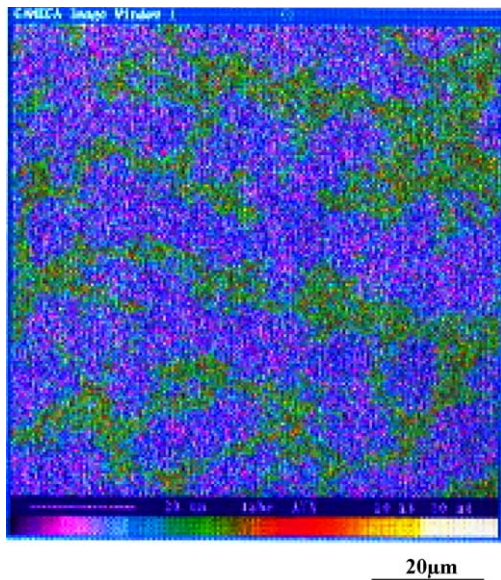


Fig. 3. Mn X-ray map from $\text{Fe}_{16.7}\text{Cr}_{16.7}\text{Mn}_{16.7}\text{Ni}_{16.7}\text{Co}_{16.7}\text{Nb}_{16.7}$.

Table 2
Lattice parameters of dendritic fcc and interdendritic bcc phases (nm)

Alloy	fcc	bcc
FeCrMnNiCo	0.359	
Nb	0.362	
Ge	0.358	0.229
Cu	0.359	
Ti	0.364	0.482
V	0.358	

and 290 kg/mm^2 , respectively, in FeCrMnNiCo. The dendrite hardness was similar to FeCrMnNiCo in the Ge and Cu alloys, but increased sharply to approximately 1000 kg/mm^2 in the Nb, Ti and V alloys. The interdendritic hardness was similar to FeCrMnNiCo in the Nb, Cu and V alloys, but increased sharply to approximately 650 and 1000 kg/mm^2 in the Ti and Ge alloys, respectively.

Similar features were found in six component alloys with different sixth alloying additions to FeCrMnNiCo, and were also found in seven, eight and nine component alloys with various combinations of additional alloying additions. The alloys all solidified with fcc primary dendrites, interdendritic segregation and one or two interdendritic phases.

Table 3
Average dendritic and interdendritic microhardness values (kg/mm^2)

Alloy	Dendrite	Interdendritic
FeCrMnNiCo	300	290
Nb	1031	399
Ge	298	1068
Cu	310	314
Ti	998	643
V	1007	287

4. Discussion

Multicomponent alloy phase space contains an extensive single fcc phase field for late transition metal rich compositions. An extensive glass forming phase field and an extensive Laves phase field have recently been found in early transition metal rich multicomponent alloys [1]. The fcc phase field includes the composition $\text{Fe}_{20}\text{Cr}_{20}\text{Mn}_{20}\text{Ni}_{20}\text{Co}_{20}$, and is capable of dissolving substantial amounts of Nb, Ti and V, as well as smaller amounts of Cu and Ge. It presumably extends to include the fcc austenite phase in pure Fe, pure Ni and binary Fe–Ni alloys. The multicomponent fcc lattice parameter is in the range 0.358–0.364 nm, and increases with incorporation of larger atoms such as Nb and Ti. This is similar to the Fe fcc lattice parameter of 0.357 nm, and somewhat higher than the Ni fcc lattice parameter of 0.352 nm. It is somewhat surprising that fcc austenite can dissolve such large amounts of elements such as Cr, Mn, Co and particularly Nb and Ti which are not fcc. More electronegative elements such as Ge and Cu show considerably less solubility. In Pd-based binary alloys, it has been shown that solutes that reduce the number of valence electrons per atom stabilize an fcc solid solution because of a negative structure-dependent enthalpy [2].

The morphology, size and hardness of the dendrites are sensitive to alloying content. Highly regular dendrites in $\text{Fe}_{20}\text{Cr}_{20}\text{Mn}_{20}\text{Ni}_{20}\text{Co}_{20}$ are refined in size with additions of Ge and Cu, and become more rounded and irregular with additions of Nb and Ti. $\text{Fe}_{20}\text{Cr}_{20}\text{Mn}_{20}\text{Ni}_{20}\text{Co}_{20}$ has a microhardness of approximately 300 kg/mm^2 , which is increased substantially with additions of Nb, Ti and V.

The Gibbs phase rule gives the maximum number of equilibrium phases as $p = c + 1$ in a c component system at constant pressure. The maximum number of phases can be greater under non-equilibrium conditions such as during casting or melt spinning, i.e. in general $p > c + 1$. The late transition metal rich multicomponent alloys described above all solidify dendritically to form a majority fcc primary dendritic phase, with interdendritic segregation, and sometimes additional interdendritic phases. The total number of phases is always well below the maximum equilibrium number allowed by the Gibbs phase rule, and even further below the maximum number allowed under non-equilibrium solidification conditions. It is often claimed that glass formation is favoured in multicomponent alloy systems because of a confusion principle, with different sized and chemically dissimilar atoms hindering the process of crystallization [3]. The multicomponent alloys described above do not form metallic glasses during casting or melt spinning. The difference in atomic radius between each component is less than 15% [4] and would therefore be expected to form a solid solution according to Hume–Rothery Rule [5] on substitutional solid solutions. Hence, the confusion principle does not apply in this case, and other factors are more important in promoting glass formation.

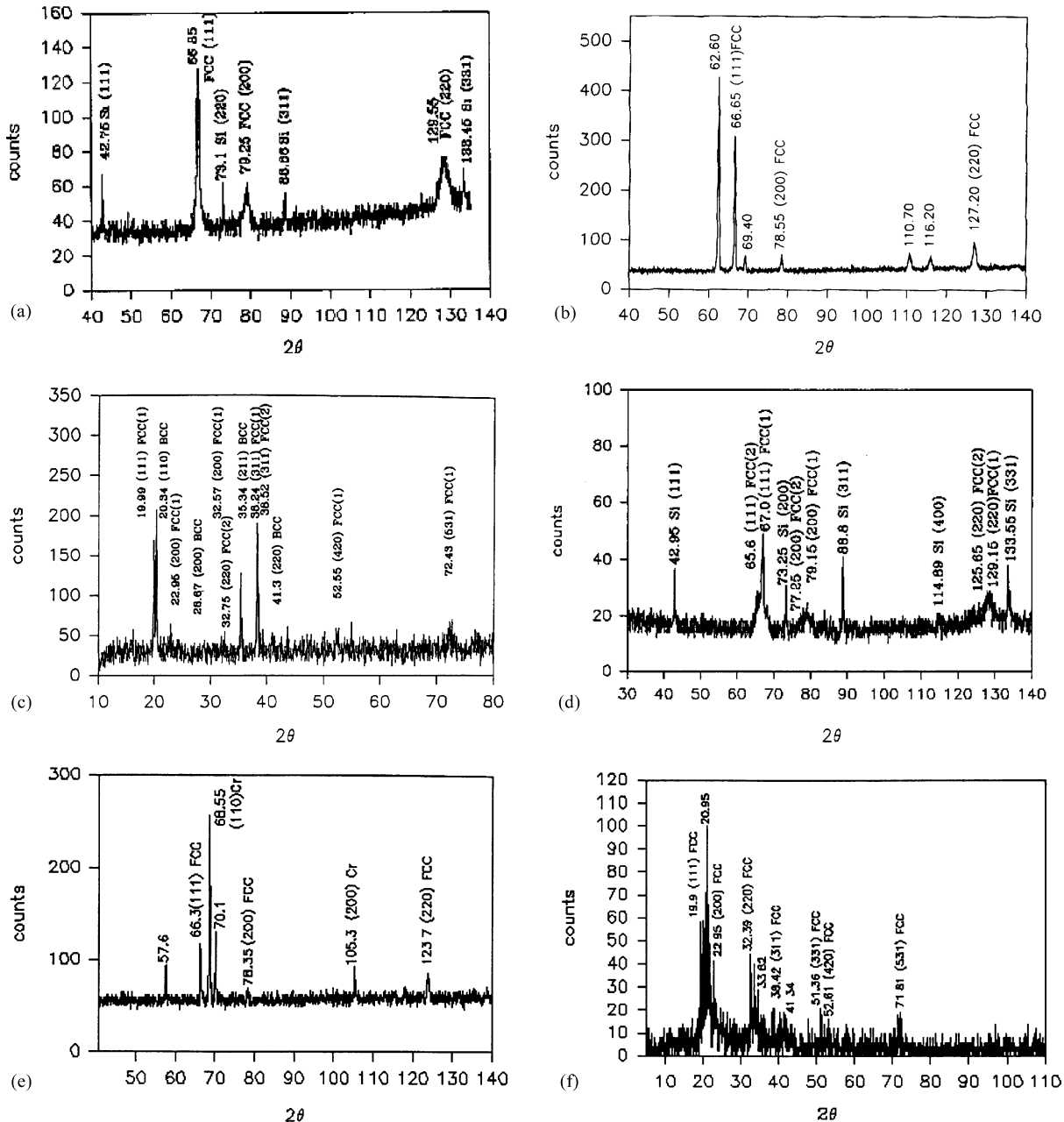


Fig. 4. X-ray diffraction patterns from: (a) Fe₂₀Cr₂₀Mn₂₀Ni₂₀Co₂₀; (b) Fe_{16.7}Cr_{16.7}Mn_{16.7}Ni_{16.7}Co_{16.7}Nb_{16.7}; (c) Fe_{16.7}Cr_{16.7}Mn_{16.7}Ni_{16.7}Co_{16.7}Ge_{16.7}; (d) Fe_{16.7}Cr_{16.7}Mn_{16.7}Ni_{16.7}Co_{16.7}Cu_{16.7}; (e) Fe_{16.7}Cr_{16.7}Mn_{16.7}Ni_{16.7}Co_{16.7}Ti_{16.7}; and (f) Fe_{16.7}Cr_{16.7}Mn_{16.7}Ni_{16.7}Co_{16.7}V_{16.7} obtained using Cr source with V filter (a, b, d, e) and Mo source with Zr filter (c and f).

5. Conclusions

Alloys containing 16 and 20 components in equal proportions are multiphase, crystalline and brittle both as-cast and after melt spinning. A five component Fe₂₀Cr₂₀Mn₂₀Ni₂₀Co₂₀ alloy forms a single fcc solid solution which solidifies dendritically. A wide range of other six to nine component late transition metal rich multicomponent alloys exhibit the same majority fcc primary dendritic phase, which can dissolve substantial amounts of other transition metals such as Nb, Ti and V. More elec-

tronegative elements such as Cu and Ge are less stable in the fcc dendrites and are rejected into the interdendritic regions. The total number of phases is always well below the maximum equilibrium number allowed by the Gibbs phase rule, and even further below the maximum number allowed under non-equilibrium solidification conditions. Glassy structures are not formed by casting or melt spinning late transition metal rich multicomponent alloys, indicating that the confusion principle does not apply, and other factors are more important in promoting glass formation.

Acknowledgements

The authors would like to thank Chris Salter for the help with the EPMA facility.

References

- [1] B. Cantor, K.B. Kim, P.J. Warren, Mater. Sci. Forum 386–388 (2002) 27.
- [2] F.R. De. Boer, R. Boom, W.C.M. Mattens, A.R. Miedema, A.K. Niessen, in: Cohesion in Metals, North Holland, 1988, p. 82.
- [3] A. Inoue, Sci. Rep. RITU A2 (1996) 1.
- [4] D.M. Considine, Van Nostrands Scientific Encyclopedia, eighth ed., International Thomson Publishing Ltd., 1995, p. 633.
- [5] A.H. Cottrell, An Introduction to Metallurgy, Edward Arnold Publishing Limited, 1971, p. 192.